The EMBO Journal vol.8 no.13 pp.4307-4314, 1989

Conformational alterations in the *ermC* transcript *in vivo* during induction

Mark Mayford and Bernard Weisblum[1]

Department of Molecular Biology, University of Wisconsin, Madison, WI 53706 and Department of Pharmacology, University of Wisconsin Medical School, Madison, Wisconsin, 53706, USA

Communicated by S.D.Ehrlich

[1]Corresponding author

***ermC* is an inducible antibiotic resistance gene from *Staphylococcus aureus*, one of several whose expression is regulated at the level of mRNA secondary structure. During induction of *ermC*, the inhibition of a ribosome active in translation of a short leader peptide by low levels of antibiotic belonging to the macrolide-lincosamide-streptogramin B family is believed to cause a rearrangement in mRNA secondary structure. The resultant conformational isomerization unmasks the methylase ribosome binding site and initiator Met codon, causing increased translation of the *ermC* transcript. Expression of *ermC* can also be demonstrated in *Bacillus subtilis* carrying plasmid pE194. To probe the *ermC* transcript *in vivo* during induction, *ermC* was transferred to *B.subtilis* by transformation and the resultant transformants were treated with dimethyl sulfate which reacts with N-1 of adenine and N-3 of cytosine residues in a manner that is sensitive to secondary structure. The bases modified *in vivo* were detected by primer extension with reverse transcriptase using total cellular RNA as template and a complementary *ermC*-specific oligonucleotide as primer. Physical evidence was obtained for the secondary structural rearrangements predicted by the *ermC* regulatory model. Additionally, physical evidence was obtained demonstrating that during induction, the stalled ribosome protects codons 9 and 10 of the leader peptide from modification by dimethyl sulfate, in agreement with genetic data obtained previously that identified the integrity of codons 5-9 as critical for induction of *ermC* by erythromycin.**

Key words: antibiotics/*Bacillus subtilis*/*ermC*/induction

Introduction

The regulation of gene expression post-transcriptionally can occur at the level of translational efficiency or physical stability of a given transcript. Examples of post-transcriptional regulation in both prokaryotic and eukaryotic organisms have been described in which modulation of mRNA secondary structure affects the stability or translatability of the transcript (Gryczan *et al.*, 1980; Horinouchi and Weisblum, 1980; Altuvia *et al.*, 1987; Müllner and Kühn, 1988). We have studied the inducible changes in mRNA structure associated with expression of *ermC* from *Staphylococcus aureus* and devised means to demonstrate the changes as they occur *in vivo*.

The *ermC* gene encodes an inducible rRNA methylase that confers resistance to the macrolide-lincosamide-streptogramin B group of prokaryotic translation inhibitors. Exposure of cells containing *ermC* to nanomolar concentrations of erythromycin (Em), a macrolide antibiotic, results in about a 10-fold increase in the intracellular level of methylase protein during a 60 min period (Shivakumar *et al.*, 1979). A model for regulation of *ermC* has been proposed and is outlined in Figure 1 (Gryczan *et al.*, 1980; Horinouchi and Weisblum, 1980). According to the model, *ermC* mRNA is transcribed constitutively but only small amounts of methylase protein are produced due to sequestration of the methylase ribosome binding site and initiator Met codon by mRNA secondary structure (Figure 1A and B). In the presence of Em, an antibiotic-bound ribosome is thought to stall while translating the 19 amino acid leader peptide located upstream from the methylase coding region. Genetic studies suggest that the Em-bound ribosome stalls at leader peptide codon 9 (Mayford and Weisblum, 1989), as shown in Figure 1C. The stalled ribosome is believed to cause the *ermC* transcript to assume the alternative conformation shown in Figure 1C in which the methylase translation initiation sequence remains unpaired and ribosomes are able to initiate methylase translation at a higher rate. The *ermC* transcript is also physically stabilized in the presence of Em (Bechhofer and Dubnau, 1987); however, the contribution of stabilization to induced expression of *ermC* remains unclear since Narayanan and Dubnau (1987a) reported that *ermC* appeared to be functionally inducible *in vitro* under conditions that did not produce transcript stabilization. Moreover, Sandler and Weisblum (1988) in studies of the related gene, *ermA*, showed that enhancement of mRNA stabilization in response to Em added to the culture did not result in enhanced gene expression.

Previous studies of the *ermC* transcript *in vitro* using enzymatic probes of RNA secondary structure provided a static picture of the conformation of the transcript that was consistent with the structures shown in Figure 1 (Mayford and Weisblum, 1985; Narayanan and Dubnau, 1985). However, *in vitro* methods cannot be used to demonstrate the Em-induced conformational transition in the *ermC* transcript that comprises the critical regulatory event in translational attenuation. We have used dimethyl sulfate (DMS) to probe, *in vivo*, both the *ermC* transcript and two mutants of *ermC* that are no longer inducible by Em due to alterations in the leader peptide coding sequence. Following treatment of growing cells with DMS, the bases modified *in vivo* were detected by primer extension with reverse transcriptase using total cellular RNA as template and a complementary *ermC*-specific oligonucleotide primer. The DMS modification profiles provide physical evidence

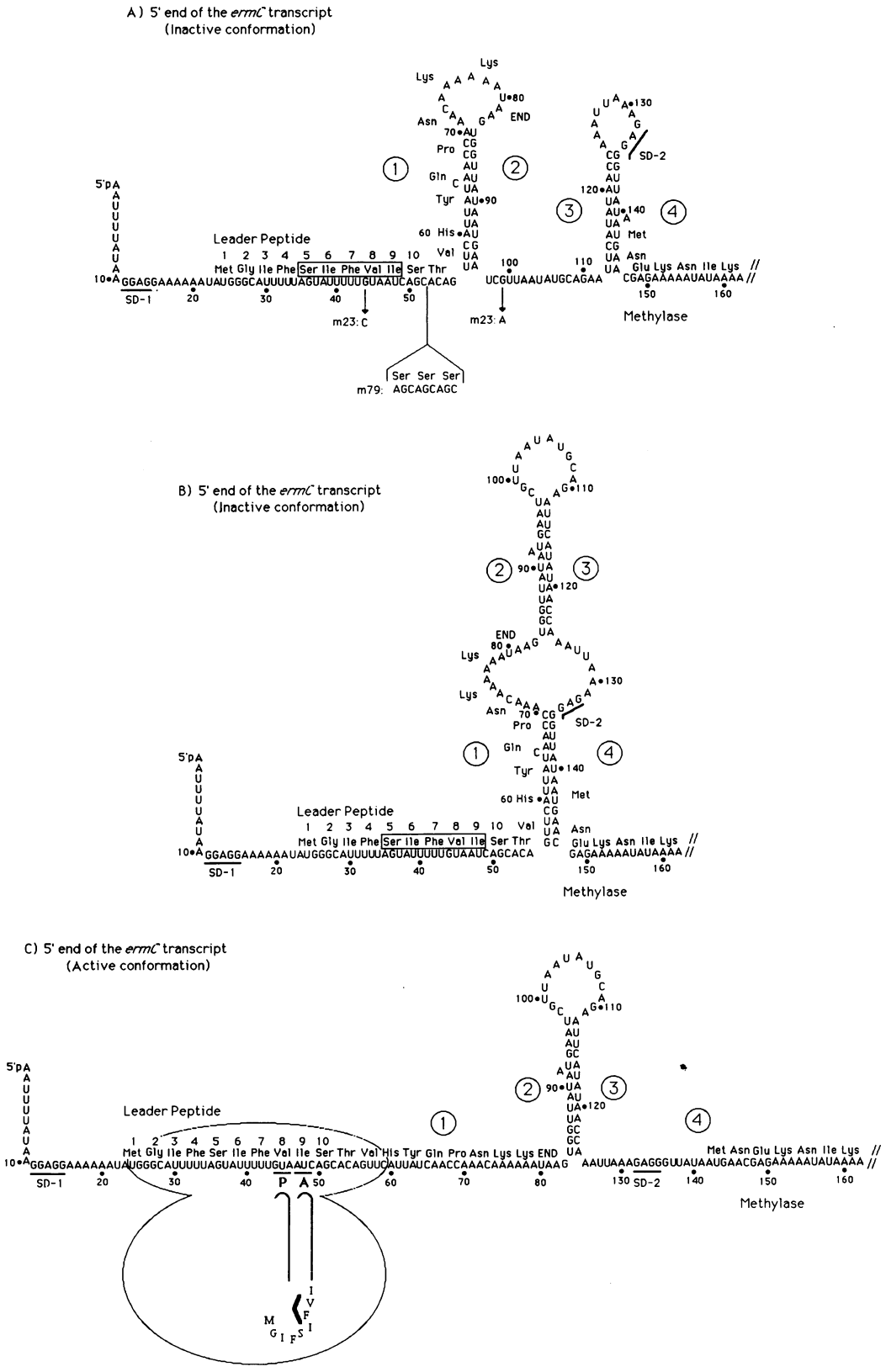

Fig. 1. Structure of the 5′ end of the *ermC* transcript. (**A**) Nucleotide sequence and predicted secondary structure of the 5′ end of the translationally inactive form of the *ermC* transcript. Translation of the boxed amino acids is critical for Em-induced expression of *ermC*. Sequence alterations associated with two non-inducible mutants, m23 and m79, are indicated. SD-1 and SD-2 refer to the ribosomal binding sites for translation initiation of the leader peptide and methylase respectively. 1, 2, 3 and 4 denote segments of the transcript capable of forming stem−loop structures by intramolecular base pairing. (**B**) Alternate, inactive conformation of the *ermC* transcript. (**C**) Predicted structure of the translationally active form of the *ermC* transcript. The transcript is shown with an Em-bound ribosome 'stalled' at the position suggested by previous genetic analysis (Mayford and Weisblum, 1989).

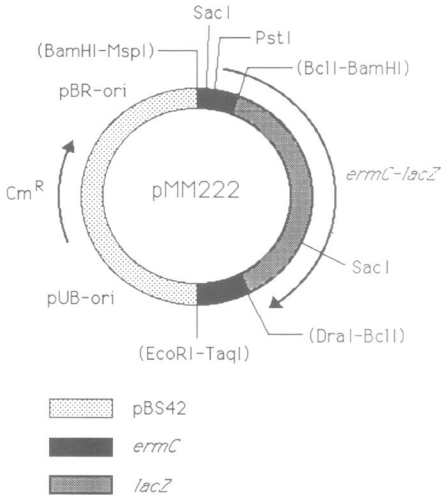

Fig. 2. Schematic diagram of pMM222. The plasmid contains the pC194 chloramphenicol resistance gene (Cm^R), replication functions for both *E.coli* and *B.subtilis*, and an in-phase translation fusion of the pE194 *ermC* methylase with *E.coli* β-galactosidase. The restriction sites shown in parentheses are not present as such in pMM222, but represent the boundaries between the different DNA fragments used in its construction.

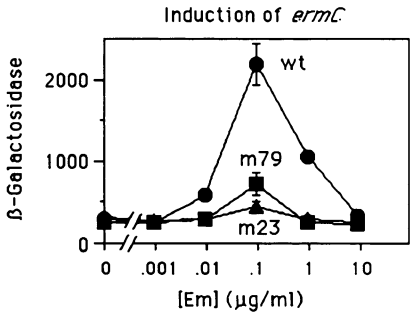

Fig. 3. Induction of *ermC* mutants. Concentration dependence for Em-induced expression of the *ermC* wild-type and leader peptide mutants. β-Galactosidase activity is expressed in Miller units (Miller, 1972).

that demonstrates the critical events, namely ribosome stall and mRNA structural rearrangement, as they occur *in vivo* during induced *ermC* expression.

Results

ermC mutants

Plasmid pMM222 (Figure 2) carrying the *ermC* regulatory region as part of an *ermC*−*lacZ* translational fusion was described previously (Mayford and Weisblum, 1989). Two regulatory mutants of *ermC* (Figure 1A) which were no longer inducible by Em were studied, in addition to wild-type *ermC*. Non-inducible mutant m23 carries a substitution at nucleotide G44 that changes leader peptide codon 86 from GUA-Val to CUA-Leu. This substitution is postulated to eliminate the ability of Em to induce *ermC* by altering a critical region of the *ermC* leader peptide (boxed amino acid sequence in Figure 1A) so that Em-bound ribosomes do not stall during leader peptide translation (Mayford and Weisblum, 1989). A second substitution not noted previously in mutant m23, at nucleotide G99, would not be expected to affect *ermC* regulation since it is located within the region between stem segments 2 and 3, where we have previously made substitutions without producing detectable changes in regulation (M.Mayford, unpublished result). Mutant m79, constructed as described previously (Mayford and Weisblum, 1989), contains a 9-base insertion $(AGC)_3$ between leader peptide codons Ser-10 and Thr-11 which reduced the inducibility by Em from 8-fold to 3-fold (Figure 3). The leader peptide codons critical for ribosome stall remain unaltered in mutant m79 but are displaced upstream from stem segment 1. We expect that in this mutant, Em would induce ribosomes to stall too far upstream from stem segment 1 to disrupt 1:2 pairing directly and thereby cause the conformational isomerization necessary for increased *ermC* expression.

In vivo DMS modification

Selective modification of unpaired bases in RNA, coupled with reverse transcription to detect the modified bases, have been used to study RNA secondary structure and RNA−protein interactions *in vitro* (Inoue and Cech, 1985; Moazed *et al.*, 1986). We tested the ability of three chemical probes [1-cyclohexyl-3-(2-morpholinoethyl)-carbodiimide metho-*p*-toluene-sulfonate, DMS and kethoxal] to modify the *ermC* transcript *in vivo* in *B.subtilis*. All three agents modified the transcript *in vitro*; however, only DMS produced detectable levels of modification *in vivo* (M.Mayford, unpublished observation). The ability of DMS to modify DNA *in vivo* at the N-7 position of guanine residues was demonstrated previously (Nick and Gilbert, 1985; Becker *et al.*, 1987). DMS methylates the N-1 position of cytosine and N-3 position of adenine residues if those positions are not blocked by Watson−Crick base pairing or interaction with proteins, ribosomes, etc. (Inoue and Cech, 1985; Moazed *et al.*, 1986). Thus, DMS treatment allows us to monitor the accessibility of A and C residues of a given transcript *in vivo*.

In a typical experiment, *B.subtilis* carrying either the wild-type or mutant *ermC* regulatory region was grown to mid-log phase, and antibiotic was added to a portion of the culture. The cells were then exposed to DMS for 5 min, and total RNA was isolated. Extension of either of two *ermC*-specific oligonucleotide primers with reverse transcriptase was used both to detect DMS-methylated bases and to generate a dideoxy sequencing ladder using control RNA that was not treated with DMS. Since the *ermC* transcript is also stabilized in the presence of Em (Bechhofer and Dubnau, 1987) and the same amount of total RNA was added to each primer extension reaction, the amount of *ermC*-specific transcript synthesized varied between Em-treated and untreated samples. To adjust for this variation, preliminary polyacrylamide gel fractionation and autoradiography were performed, after which the samples were diluted to give approximately equal intensities for an arbitrarily chosen set of bands that were used as internal standards. In the case of primer extension using oligo T161 (Figures 4A and 6A), the internal standard bands corresponded to nucleotides A71−A78, located within the proposed looped region between stem segments 1 and 2 (Figure 1A). When using oligo T219 (Figures 4B and 6B), nucleotides A151−A155, located just downstream from stem segment 4 within the methylase coding region, were used for normalization.

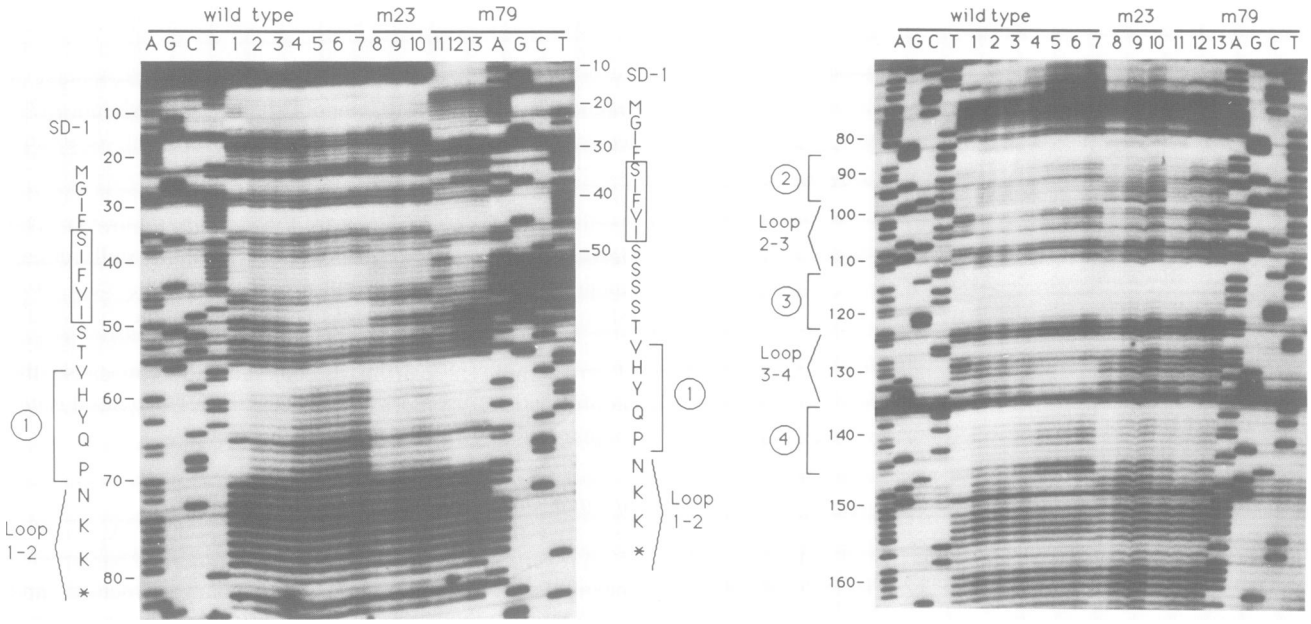

Fig. 4. Reverse transcription analysis of *ermC* transcripts modified with DMS *in vivo* during induction. **(A)** Primer extension using oligo T161. **(B)** Primer extension using oligo T219. A, G, C and T are dideoxy sequencing reactions using RNA which was not treated with DMS. **Lane 1**: wild-type *ermC* transcript modified *in vitro*. **Lanes 2–7**: wild-type *ermC* transcript treated with DMS *in vivo* using 0, 0.001, 0.01, 0.1, 1 and 10 μg/ml Em respectively for induction. **Lanes 8–10**; mutant m23 in the presence of 0, 0.1 and 1 μg/ml Em respectively. **Lanes 11–13**: mutant m79 in the presence of 0, 0.1 and 1 μg/ml Em respectively.

DMS modification of the Em-induced ermC transcript

Nucleotides A1–U58 (pre-stem segment 1, leader peptide coding sequence). The *in vivo* DMS modification profile of the wild-type *ermC* transcript in the presence of increasing amounts of Em is shown in Figure 4A, lanes 2–7. The extent of DMS modification of the majority of nucleotides (A1–U58) was unaffected by added Em. However, the reactivity of nucleotides A46–C52 toward DMS decreased with increasing concentrations of Em for both the wild-type and mutant m79 (lanes 2–7 and 11–13 respectively), whereas those same nucleotides remained unaffected following addition of Em in mutant m23 (lanes 8–10). These results are summarized quantitatively in Figure 5A, using nucleotides A71–A78 as internal standards. The DMS accessibility of nucleotides A46–C52 became minimal at the same Em concentration, 0.1 μg/ml, that induced *ermC* expression maximally (cf. Figure 3 and Figure 5A). We believe that the protection of nucleotides A46–C52 from DMS modification is due to the presence of an Em-bound ribosome on the wild-type and mutant m79 transcripts.

Nucleotides C59–G83 (stem segment 1 and stem loop 1:2). Nucleotides C59–C69, located within stem segment 1, were weakly modified by DMS in the absence of added Em (with the exception of nucleotide C65 which is predicted to remain unpaired in stem–loop 1:2) but showed increased reactivity in the presence of Em. In the two non-inducible mutants, m23 and m79 (lanes 8–10 and 11–13 respectively), nucleotides in stem segment 1 remained inaccessible to DMS in the presence of Em. These results are summarized quantitatively in Figure 5B, using nucleotides A71–A78 as internal standards. Nucleotides A70–G83, within the proposed looped region between stem segments 1 and 2 were strongly modified by DMS irrespective of added Em. The Em concentration dependence of increased DMS modification of stem segment 1 paralleled that of the reduced modification of nucleotides A46–C52, which is postulated to result from Em-induced ribosome stall (cf. Figure 5A and B). Lane 1 in Figure 4A and B shows results obtained with *ermC* mRNA modified by DMS *in vitro*. Total RNA from untreated cells was DMS modified *in vitro*, as described previously (Moazed and Noller, 1986), and analyzed using *ermC*-specific primers. The modification profile resembled that of the *in vivo* modified transcript obtained in the absence of antibiotic (lane 2), except that stem segment 1 appeared to be more accessible to DMS *in vivo* than *in vitro*.

Nucleotides U84–G134 (stem segments 2 and 3). The DMS-accessibility profile of the *ermC* transcript in the region of stem segments 2–4 is shown in Figure 4B. The bands that were used as internal standards correspond to nucleotides A151–A155, located just within the *ermC* methylase coding region. Stem segment 2, nucleotides U84–A96, was relatively inaccessible to DMS under all conditions. However, increased band strength at nucleotides A91, A92 and G94 and a decrease in intensity at nucleotides G85 and G86 was seen in the presence of Em in both the wild-type and mutant m79. The region between stem segments 2 and 3 (loop 2:3), nucleotides U97–A112, showed a high level of DMS modification. Several nucleotides within this region show increased accessibility to DMS in the presence of Em in both the wild-type and in mutant m79. While the relative DMS accessibility of loop 2:3 did not change in the presence of Em for mutant m23, a strong band at nucleotide 99 was seen which was absent in the wild-type and was attributable to the substitution of adenine at nucleotide G99. In all samples, nucleotides U113–C123, within stem segment 3, showed little or no reactivity with DMS. Nucleotides A124–A133, located within the region between stem segments 3 and 4 (loop 3:4), were readily modified by DMS, and this modification was slightly reduced by added Em, possibly reflecting the increased utilization of the ribosome binding site for methylase synthesis.

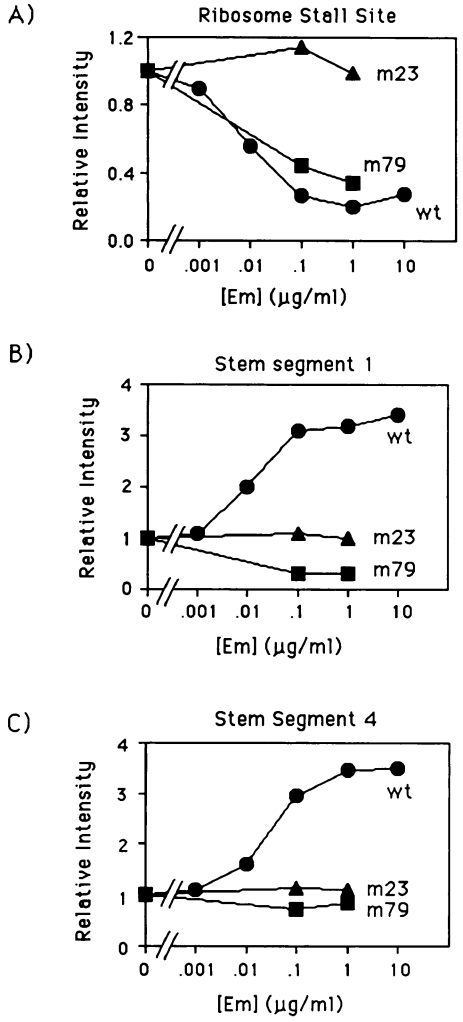

Fig. 5. Densitometric quantitation of *ermC* mRNA modification by DMS. (**A**) Average density change over the putative ribosome stall site (nucleotides A46–A52) as a function of Em concentration. (**B**) Average density change over stem segment 1 (nucleotides C59–C69) as a function of Em concentration. (**C**) Average density change over stem segment 4 (nucleotides A139–U142 and A145–A146) as a function of Em concentration. Nucleotides A71–A78 (panels A and B) or nucleotides A151–A155 (panel C) served as internal standards to allow comparison between individual lanes. Changes are expressed relative to the 0 Em sample.

Nucleotides G135–A146 (stem segment 4). In the wild-type samples (lanes 2–7) nucleotides within stem segment 4, A139–U142 and A145–A146, showed increased accessibility to DMS in the presence of Em, whereas the accessibility of these same nucleotides to DMS remained unaltered by added Em in the two non-inducible mutants, m23 and m79. These results are summarized quantitatively in Figure 5C, using nucleotides A151–A155 as internal standards. The concentration of Em at which stem segment 4 became maximally accessible to DMS modification was the same as that of stem segment 1 and of maximal induced gene expression (cf. Figure 5C with Figure 5B and Figure 3). Lane 1 shows the ladder obtained when the *ermC* transcript was modified *in vitro* with DMS. The modification profile is comparable to *in vivo* modification in the absence of antibiotic (lane 2) except that stem segments 2–4 appear less accessible to DMS *in vitro* than *in vivo*.

Effects of other translation inhibitors on the ermC transcript

Only a subset of the antibiotics which inhibit prokaryotic translation has been found to induce expression of *ermC*. We therefore tested the effect of 11 antibiotics on DMS modification of the *ermC* transcript *in vivo* (Figure 6). Only four of these antibiotics induce *ermC* expression, namely Em, Megalomicin (Meg), Celesticetin (Cel) and Oleandomycin (Ole), and these also were the only antibiotics in the group of 11 tested that produced the altered pattern of DMS modification, characterized by enhanced accessibilty of stem segments 1 and 4 and reduced accessibility of nucleotides A46–C52. Thus, the ability of an antibiotic to alter the *in vivo* DMS accessibility profile of the *ermC* transcript is correlated with its ability to induce gene expression.

Discussion

We have used DMS to demonstrate the *in vivo* mRNA structural rearrangement associated with induced expression of *ermC* in *B.subtilis*. The technique is rapid and requires only a knowledge of the sequence within the region to be analyzed. The use of DMS *in vivo* allows analysis of specific transcripts under biologically active conditions as well as the observation of induced structural transitions due to changes in external conditions.

DMS has been shown to methylate the N-1 position of cytosine, the N-3 position of adenine and the N-7 position of guanine residues (reviewed by Singer and Grunberger, 1983). The reverse-transcriptase reaction terminates (or pauses) at 1-methylcytosine and 3-methyladenine, but not at 7-methylguanine (Hagenbüchle *et al.*, 1978; Youvan and Hearst, 1979). We have noted, however, termination at certain G and U positions following DMS treatment (see Figure 4). Terminations at G are generally weak and occur only when DMS modification is performed *in vivo*. This observation may reflect the formation of a ring-opened derivative of 7-methylguanine previously found in cells treated with alkylating agents (Beranek *et al.*, 1983). This type of derivative has been shown to produce chain termination in primer extension reactions using T4 DNA polymerase (O'Connor *et al.*, 1988). The U terminations are also weak but occur both *in vivo* and *in vitro* and appear to be sensitive to RNA secondary structure. Similar DMS-induced weak terminations at U residues have been noted previously (Moazed and Noller, 1986; Svensson *et al.*, 1988). DMS is able to methylate the N-3 position of uridine nucleotides *in vitro* (Singer, 1975); however, 3-methyluridine is not detected when DMS-modified polynucleotides are examined (Singer and Grunberger, 1983). It is possible that the U terminations represent weak methylation of the N-3 position. Since the N-3 position of U is involved in Watson–Crick base pairing, modification at this position would be both sensitive to secondary structure and likely to cause termination of polymerization by AMV reverse transcriptase.

The *ermC* regulatory model predicts that in the presence of inducing levels of antibiotic, the 5′ end of the *ermC* transcript undergoes a transition from the structure(s) shown in Figure 1A and B to the structure in Figure 1C (Gryczan *et al.*, 1980; Horinouchi and Weisblum, 1980). The *in vivo* DMS modification profile of the *ermC* transcript is consistent with this prediction. In the absence of antibiotic, the

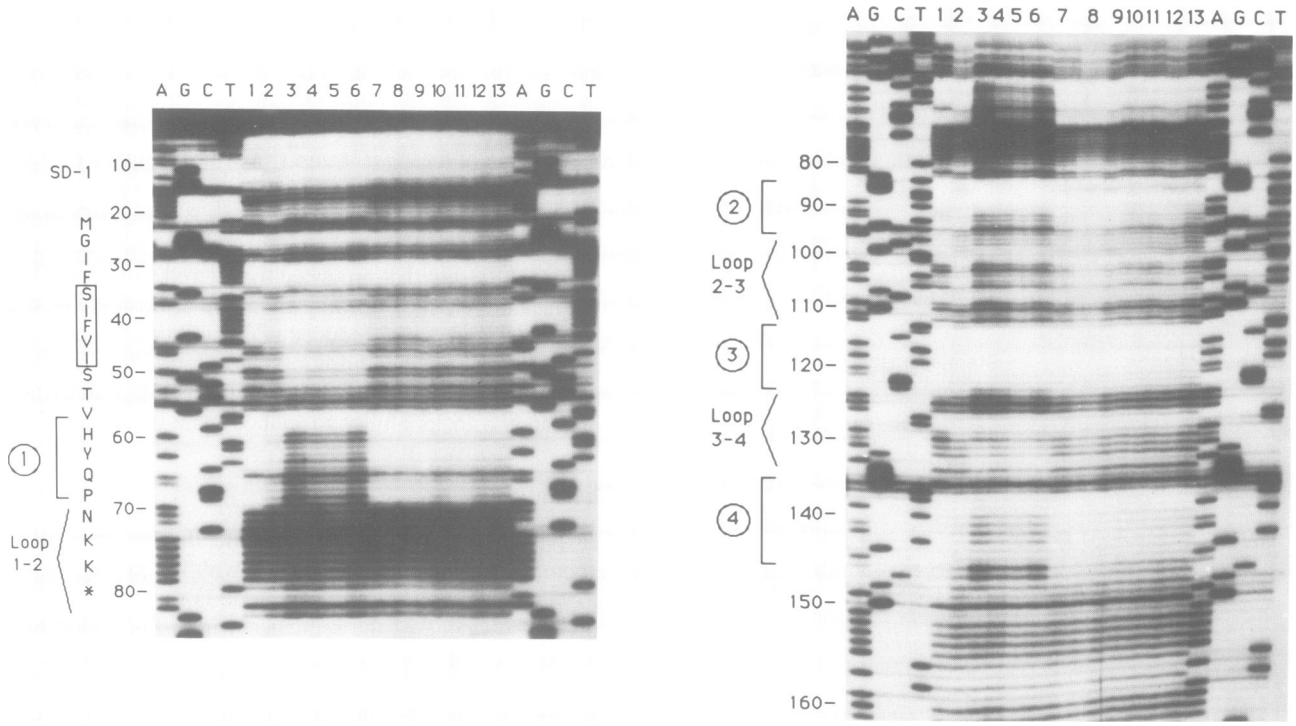

Fig. 6. *In vivo* DMS accessibility of the wild-type *ermC* transcript in the presence of various antibiotics. (**A**) Primer extension using oligo1. (**B**) Primer extension using oligo2. A, G, C and T are RNA sequencing lanes. **Lane 1**: wild-type *ermC* transcript modified *in vitro*. **Lanes 2–13**: *in vivo* DMS modification of the *ermC* transcript in the presence of **2**, no antibiotic; **3**, 10 μg/ml Em; **4**, 10 μg/ml celesticetin; **5**, 30 μg/ml megalomicin; **6**, 10 μg/ml oleandomycin; **7**, 10 μg/ml tylosin; **8**, 10 μg/ml maridomycin; **9**, 10 μg/ml lincomycin; **10**, 10 μg/ml staphylomycin S; **11**, 10 μg/ml tetracycline; **12**, 10 μg/ml neomycin; **13**; 10 μg/ml fluorothiamphenicol.

nucleotides in stem segments 1–4 are relatively inaccessible to DMS, suggesting that they are involved in intramolecular base pairing. However, after exposure of cells to levels of antibiotic that induce gene expression, stem segments 1 and 4 showed greater accessibility to DMS attack than stem segments 2 and 3 which remained relatively unchanged. Comparison of stem segments 2 and 3 (Figure 4B) suggests that segment 3 may be less susceptible to methylation than segment 2. The reasons for this difference are unclear. These observations are consistent with a transcript configured as shown in Figure 1A or B undergoing a transition to the conformation shown in Figure 1C, in which stem segments 1 and 4 become unpaired during induction, whereas stem segments 2 and 3 remained base paired. Altered DMS accessibility of stem segments 1 and 4 is clearly correlated with induced gene expression. The changes in DMS accessibility are associated only with the translation inhibitors that induce *ermC* (Em, Ole, Meg, Cel) and not with any of seven other non-inducing antibiotics tested. Also, these changes occur only in the wild-type *ermC* transcript and not in the transcripts of non-inducible mutants m23 and m79. The low level of inducibility of mutant m79 (~3-fold) in the absence of any alteration in stem segment 4 may be due to the enhanced stability of the m79 transcript in the presence of Em (M.Mayford, unpublished results). Although it has been shown that Em-induced stabilization of a transcript does not necessarily result in increased levels of protein synthesis (Sandler and Weisblum, 1988), recent results suggest that the effect may be transcript specific (Sandler and Weisblum, 1989).

The reactivity of stem segments 1 and 4 with DMS reaches a maximum at ~0.1 μg/ml Em and remains maximal up to 10 μg/ml, the highest concentration tested. Induced expression of *ermC* is also maximal at 0.1 μg/ml Em, but at higher concentrations of Em, expression is reduced, even though our findings suggest that the transcript remains in the active conformation. It is likely that this observation reflects competition between the inhibitory effect of the antibiotic on protein synthesis and its ability to alter mRNA conformation. At higher levels of antibiotic, the inhibitory effect of Em on methylase synthesis overrides the enhancement of methylase translation initiation caused by the mRNA structural rearrangement. Thus, the Em concentration that optimally induces gene expression corresponds to the minimum concentration that fully converts the mRNA to the translationally active form.

Accessibility of the stem segments of the *ermC* transcript to DMS appears to be less *in vitro* than *in vivo*, as shown in Figure 4, lanes 1 and 2. A possible explanation is that differences in ionic conditions *in vivo* versus *in vitro* result in differences in the stability of the mRNA secondary structures. We expect that the leader peptide is actively translated *in vivo* and that this will result in repeated disruption and reformation of stem 1:2. This 'ribosome traffic' may account for the increased DMS accessibility of stem segment 1. Consistent with this interpretation is the observation that Em induces a decrease in DMS accessibility of stem segment 1 in mutant m79. The presence of an Em-bound ribosome upstream from stem segment 1 in mutant m79 might be expected to block downstream ribosome traffic and allow tighter pairing of stem segment 1. If this were the case, we would also predict an Em-induced decrease in stem segment 2 accessibility to DMS in mutant m79. Stem segment 2 of mutant m79 shows Em-induced increases in

band intensity at nucleotides A91, A92 and G94 as well as decreased intensity at G85 and G86. The wild-type *ermC* transcript shows a similar Em-induced change in the banding pattern of stem segment 2. These alterations in DMS accessibility may reflect a transition from a conformation in which stem segment 2 is base paired with stem segment 1 to one in which stem segment 2 is paired with stem segment 3 (Figure 1B and C).

In the 2:3 pairing scheme, either nucleotide A91 or A92 is predicted to remain unpaired and may thus react with DMS to a greater extent than the neighboring base-pairing nucleotides. In mutant m79, Em-induced block of ribosome traffic within stem segments 1 and 2 may allow conversion of the transcript to a structure in which stem segments 2:3 and 1:4 are paired (Figure 1B; Mayford and Weisblum, 1989). The increased DMS modification of stem segment 4 *in vivo* cannot be ascribed to ribosome traffic within the leader peptide coding sequence since this modification is not reduced by Em in mutant m79, whereas stem segment 1 modification is reduced. Since the translational attenuation model postulates that the level of *ermC* expression is inversely correlated with the extent of stem segment 4 base pairing, this observation is consistent with earlier reports that termination of leader peptide translation at the second codon did not increase the basal level of *ermC* expression (Dubnau, 1985). The cause of the increased DMS accessibility of stem segment 4 *in vivo* compared to *in vitro* is unclear, but partial unpairing of stem segment 4 in the absence of added Em is consistent with the basal level of expression observed for *ermC*.

The induced conformational changes in the *ermC* transcript are thought to result directly from an antibiotic-bound ribosome stalled within the leader peptide coding region. Just upstream from stem segment 1, we find a series of nucleotides (A46–C52) that are strongly protected from DMS attack in the presence of Em. We postulate that this protection represents the footprint of an Em-bound ribosome stalled on the *ermC* transcript. This footprint is not seen in mutant m23, in which a region of the leader peptide thought to be necessary for Em-induced ribosome stall is altered. However, the footprint is found in mutant m79 at the same position as in the wild-type. Mutant m79 contains an intact ribosome stall sequence displaced nine nucleotides upstream from stem segment 1 so that a stalled ribosome would be unable to disrupt 1:2 base pairing efficiently. Em-induced gene expression is reduced in mutant m79, and the Em-induced changes in DMS accessibility of stem segments 1 and 4 are not found. Therefore, the protection of nucleotides A46–C52 is associated with the critical sequence in the leader peptide at which the Em-bound ribosome is thought to stall, rather than with the subsequent structural rearrangement linked to induced gene expression. Mutant m79 thus enables us to dissect two key steps of the induction process, namely ribosome stall and mRNA secondary structural isomerization.

While a ribosome has been shown to protect ~35 bases of mRNA from nuclease degradation (Steitz, 1979; Kang and Cantor, 1985), it is not known how much less of that same mRNA would be protected from attack by a smaller molecule like DMS. The most strongly protected nucleotides in the *ermC* transcript, A46–C52, correspond successively to the third position of leader peptide codon Val-8 and codons Ile-9 and Ser-10. If the stalled ribosome were positioned with Ile-9 at the P-site and Ser-10 at the A-site, then the majority of the observed protection pattern could be explained by codon–anticodon pairing. The placement of the stalled ribosome at this position is consistent with previous genetic data (Mayford and Weisblum, 1989) which placed the ribosome 1 codon upstream from this position, as shown in Figure 1C.

It has been reported by Narayanan and Dubnau (1987b), using an *in vitro* translation system, that Em induces a strong cleavage in the *ermC* transcript at nucleotides A79–A81 in a nuclease protection experiment and that this cleavage represents the leading edge of an Em-bound ribosome stalled at amino acids 12–15 of the leader peptide. It is unclear what relation these results have to *ermC* regulation since previous genetic results (Mayford and Weisblum, 1989) and the present DMS protection experiments place the stalled ribosome at, or upstream from, leader peptide codon Ser-10. Since the *in vitro* induction experiments depend on an undefined nuclease activity present in the RNA preparations, the cleavages seen may reflect sensitivity of the nuclease to Em-induced conformational alterations of the *ermC* transcript, rather than the presence of a stalled ribosome.

We analyzed the effect of 11 prokaryotic translation inhibitors on the DMS accessibility profile of the *ermC* transcript. The four antibiotics which induced *ermC* expression (Em, Cel, Meg, Ole) produced alterations in the DMS accessibility of the *ermC* transcript that were indistinguishable. This suggests that Cel, Meg and Ole induce *ermC* expression in the same manner as Em, by causing ribosome stall near leader peptide codons 9 and 10 which, in turn, results in a conformational rearrangement of the transcript. Translation inhibitors could fail to activate *ermC* expression by producing ribosome stall at a point in the leader peptide which is too far upstream from stem segment 1 to disrupt stem 1:2 base pairing (the same reason postulated to explain the lack of inducibility in mutant m79). If this were the case, we would expect to see ribosome footprints on the *ermC* transcript in the presence of these antibiotics without concomitant alterations in stem segments 1 and 4 (i.e. as in mutant m79). The lack of any detectable effect of the seven non-inducing antibiotics on the leader peptide region of the *ermC* transcript suggests that either these antibiotics do not inhibit leader peptide translation or that they do so in a manner that does not allow the ribosome to remain bound to the transcript for a time sufficient to protect the transcript from DMS attack.

Materials and methods

Strains and plasmids

Bacillus subtilis BR151 (*trpC2 lys3 metB10*) was used as plasmid host in all experiments. The *ermC* promoter and attenuator were carried as part of an *ermC–lacZ* translational fusion on the wild-type derivative of plasmid pMM222 (Figure 1; Mayford and Weisblum, 1989). *ermC* regulatory mutants m23 and m79 differ from the wild-type sequence, as shown in Figure 1A. Mutant m23 is no longer inducible by Em and has been described previously (Mayford and Weisblum, 1989). Mutant m79 was constructed and its inducibility assayed as described previously (Mayford and Weisblum, 1989).

Antibiotics

The following antibiotics were obtained as gifts from pharmaceutical firms as indicated: celesticetin (The Upjohn Co.), erythromycin (Abbott Laboratories and Upjohn), fluorothiamphenicol (Schering-Plough Corporation), lincomycin (Upjohn), maridomycin (Takeda Chemical Co.),

megalomicin (Schering-Plough), oleandomycin (Chas. Pfizer Inc.), staphylomycin S (H.Vanderhaeghe) and tylosin (Eli Lilly & Co.).

In vivo DMS modification of mRNA

Cultures (20 ml) of *B.subtilis* BR151 carrying either the wild-type or mutant derivatives of pMM222 were grown at 37°C in SPII medium (Dubnau and Davidoff-Abelson, 1971) containing 10 μg/ml chloramphenicol (for plasmid selection) to mid-log phase (OD_{590} = 0.5). Antibiotic was added to each sample to the indicated concentration, and incubation was continued for 10 min. Next, 100 μl of DMS (Aldrich, Gold label) was added, followed by incubation, with vigorous shaking for 5 min at 37°C. The reaction was stopped by pouring samples onto 10 ml of frozen TME buffer (100 mM Tris−HCl, pH 7.5, 100 mM 2-mercaptoethanol, 5 mM EDTA). Cells were pelleted, washed with 1.5 ml ice-cold TSE (10 mM Tris−HCl, pH 8, 100 mM NaCl, 1 mM EDTA) and pelleted again in 1.5 ml Eppendorf tubes. Cells were resuspended in 200 μl of STET (50 mM Tris−HCl, pH 8, 8% sucrose, 0.5% Triton X-100, 10 mM EDTA) containing 4 mg/ml lysozyme and held on ice for 5 min. Samples were mixed with an equal volume of phenol/chloroform (1:1 v/v) and heated in a boiling water bath for 50 s. The phases were separated by centrifugation, and the aqueous phase was extracted once more with phenol/chloroform and once with chloroform. The RNA was precipitated with ethanol, resuspended in water to a final concentration of 2 mg/ml, and stored at −20°C.

Oligonucleotide primers

Two oligonucleotides were used to visualize the *ermC* leader region by reverse-transcriptase mapping. The oligonucleotides were named according to the first nucleotide transcribed in the *ermC* mRNA. They were, oligo T161: 5′-GAAGTAATAAAGTTTTGACTGTGT-3′, which is complementary to nucleotides 2695−2718 of the published sequence of pE194 (the plasmid from which *ermC* was initially isolated) (Horinouchi and Weisblum, 1982) corresponding to nucleotides 185−162 of the *ermC* transcript; and oligo T219: 5′-GATATTATCATGTTCATTTAATCT-3′, which is complementary to nucleotides 2637−2660 of plasmid pE194 (Horinouchi and Weisblum, 1982) corresponding to nucleotides 243−220 of the *ermC* transcript. The oligonucleotides were end-labeled before use with [γ-^{32}P]-ATP as described (Mayford and Weisblum, 1989).

Primer extension reactions

Primer extension was performed using a modification of the procedure described previously (Moazed *et al.*, 1986; Stern *et al.*, 1988). ^{32}P-end-labeled primer, 1 ng (0.13 pmol), was mixed with 5 μg of total cellular RNA in 50 mM HEPES, pH 7.0, 5 mM potassium borate, 100 mM KCl in a total volume of 7.5 μl. The mixture was heated at 70°C, slowly cooled to 42°C over 15 min and held at 42°C for 45 min. Five microliters of 2.5 × RTB (125 mM Tris−HCl, pH 8.4, 25 mM DTT, 25 mM $MgCl_2$, 500 μM each dATP, dGTP, dCTP, dTTP) containing 0.5 units/ml AMV reverse transcriptase (Life Sciences, St Petersburg, FL) was added to each sample. Reverse transcriptase was added to the 2.5 × RTB just before the reactions were started. For dideoxy sequencing reactions, 2.5 × RTB contained the appropriate dideoxy nucleotide at a concentration of 50 μM. Following incubation for 30 min at 42°C the reaction was stopped by the addition of 12 μl formamide dyes solution (Maxam and Gilbert, 1980), after which they were heated to 90°C for 1 min before loading onto 10% polyacrylamide sequencing gels.

Quantitation

Following autoradiography, band intensities were quantitated using a Zeineh Model SL-504-XL scanning densitometer (Biomed Instruments Inc., Fullerton, CA), interfaced with an Apple II microcomputer using a Zeineh D/A conversion board. Data were collected and processed using Videophoresis II software (Biomed Instruments). Intensity differences were normalized relative to a set of internal standard bands.

Acknowledgements

We thank V.Schultz for instruction on rapid RNA isolation. We also thank P.Sandler and K.Wipperfurth for critically reading this manuscript. Oligonucleotides were synthesized by the University of Wisconsin Protein Sequence−DNA Synthesis Facility supported by funds from the Public Health Service, National Institutes of Health (Shared Equipment Grant S10-RR01684, National Cancer Institute continuing support grant CA-07175 and the General Research Support Grant to the University of Wisconsin Medical School), National Science Foundation Biological Instrumentation Program, Division of Molecular Biosciences Grant DMB-8514305 and from the University of Wisconsin Graduate School. This work was supported by research grant AI-18283 from the Public Health Service, National Institutes of Health. M.M. was also supported by the National Institutes of Health Cellular and Molecular Biology training grant, T32-GM-07215.

References

Altuvia,S., Locker-Giladi,H., Koby,S., Ben-Nun,O. and Oppenheim,A.B. (1987) *Proc. Natl. Acad. Sci. USA*, **84**, 6511−6515.
Bechhofer,D.H. and Dubnau,D. (1987) *Proc. Natl. Acad. Sci. USA*, **84**, 498−502.
Becker,P.B., Ruppert,S. and Schütz,G. (1987) *Cell*, **51**, 435−443.
Beranek,D.T., Weis,C.C., Evans,F.E., Chetsanga,C.J. and Kadlubar,F.F. (1983) *Biochem. Biophys. Res. Commun.*, **110**, 625−631.
Dubnau,D. (1985) *EMBO J.*, **4**, 533−537.
Dubnau,D. and Davidoff-Abelson,R. (1971) *J. Mol. Biol.*, **56**, 209−221.
Gryczan,T.J., Grandi,G., Hahn,J., Grandi,R. and Dubnau,D. (1980) *Nucleic Acids Res.*, **8**, 6081−6097.
Hagenbüchle,O., Sante,M. and Argetsinger-Steitz,J. (1978) *Cell*, **13**, 551−563.
Horinouchi,S. and Weisblum,B. (1980) *Proc. Natl. Acad. Sci. USA*, **77**, 7079−7083.
Horinouchi,S. and Weisblum,B. (1982) *J. Bacteriol.*, **150**, 804−814.
Inoue,T. and Cech,T.R. (1985) *Proc. Natl. Acad. Sci. USA*, **82**, 648−652.
Kang,C. and Cantor,C.R. (1985) *J. Mol. Biol.*, **181**, 241−251.
Maxam,A.M. and Gilbert,W. (1980) *Methods Enzymol.*, **65**, 499−560.
Mayford,M. and Weisblum,B. (1985) *J. Mol. Biol.*, **185**, 769−780.
Mayford,M. and Weisblum,B. (1989) *J. Mol. Biol.*, **206**, 69−79.
Miller,J.H. (1972) In *Experiments in Molecular Genetics*. Cold Spring Harbor Laboratory, Cold Spring Harbor, NY, pp. 352−355.
Moazed,D. and Noller,H.F. (1986) *Cell*, **47**, 985−994.
Moazed,D., Stern,S. and Noller,H.F. (1986) *J. Mol. Biol.*, **187**, 399−416.
Müllner,E.W. and Kühn,L.C. (1988) *Cell*, **53**, 821−825.
Narayanan,C.S. and Dubnau,D. (1985) *Nucleic Acids Res.*, **13**, 7307−7325.
Narayanan,C.S. and Dubnau,D. (1987a) *J. Biol. Chem.*, **262**, 1756−1765.
Narayanan,C.S. and Dubnau,D. (1987b) *J. Biol. Chem.*, **262**, 1766−1771.
Nick,H. and Gilbert,W. (1985) *Nature*, **313**, 795−797.
O'Connor,T.R., Boiteux,S. and Laval,J. (1988) *Nucleic Acids Res.*, **13**, 5879−5894.
Sandler,P. and Weisblum,B. (1988) *J. Mol. Biol.*, **203**, 905−915.
Sandler,P. and Weisblum,B. (1989) *J. Bacteriol.*, **171**, 6680−6688.
Shivakumar,A.G., Hahn,J. and Dubnau,D. (1979) *Plasmid*, **2**, 279−289.
Singer,B. (1975) *Biochemistry*, **14**, 4353−4357.
Singer,B. and Grunberger,D. (1983) In *Molecular Biology of Mutagens and Carcinogens*. Plenum Press, New York, pp. 56−78.
Steitz,J.A. (1979) In Goldberger,R. (ed.), *Biological Regulation and Development*. Plenum Press, New York, pp. 349−399.
Stern,S., Moazed,D. and Noller,H.F. (1988) *Methods Enzymol.*, **164**, 418−489.
Sevensson,P., Changchien,L.-M., Craven,G.R. and Noller,H.F. (1988) *J. Mol. Biol.*, **200**, 301−308.
Youvan,D.C. and Hearst,J.E. (1979) *Proc. Natl. Acad. Sci. USA*, **76**, 3751−3754.

Received on June 27, 1989; revised on October 5, 1989